The Indonesian Journal of Computer Science
www.ijcs.net
Volume 13, Issue 6, December 2024
https://doi.org/10.33022/ijcs.v13i6.4447

Simulation of Voltage and Frequency Stabilization in PV-Based Microgrids Using Virtual Synchronous Generator Control

Zaw Tway Oo[1]
zawtwayoo@gmail.com[1]
[1]Ministry of Education, Naypyidaw, Myanmar

Article Information

Received : 31 Oct 2024
Revised : 8 Nov 2024
Accepted : 30 Nov 2024

Keywords

Micro-Grid System, PV Array, Virtual Synchronous Generator Control, Voltage and Frequency Stability.

Abstract

In recent years, distributed generation technologies and micro-grids have garnered increasing attention, particularly with the rapid growth of renewable energy sources (RESs) integrated via power electronic converters. As the penetration of RESs in modern power systems rises, voltage and frequency support, traditionally provided by synchronous generators, can be effectively managed by Virtual Synchronous Generator (VSG) control. This paper presents the modeling and analysis of voltage and frequency stability enhancement in a PV-based micro-grid system using VSG control. The micro-grid system under study operates at 400V, 50Hz, and is integrated with a 0.4kV power distribution line. Mathematical models of the VSG control strategy are developed in MATLAB/Simulink. Simulation results demonstrate that VSG control significantly improves the voltage and frequency stability of the PV-based micro-grid system.

A. Introduction

In recent years, Renewable Energy Sources (RESs), such as photovoltaic (PV) systems and wind turbines, have become widely adopted, playing a critical role in micro-grids. A micro-grid can be seen as a collection of controllable and distributed generation units and loads. PV systems provide consumers with a clean, silent, and dependable way to generate electricity. These systems consist of photovoltaic cells, which convert sunlight directly into electricity through the photovoltaic process [1]. Consequently, this paper centers on a PV-based microgrid system.

However, when RESs are integrated into micro-grids, they can introduce challenges such as power fluctuations, frequency deviations, and voltage instability [2]. To address these issues, three control methods are commonly employed: inverter-based control, Virtual Synchronous Machine (VSM) control, and Virtual Synchronous Generator (VSG) control. In this paper, the VSG control method is proposed, with the VSG placed between the PV source and the micro-grid, which is connected to the load [3]. In cases of power imbalance, the VSG can inject or absorb power from the system to maintain stability [4]. This paper develops and analyzes the mathematical model of the VSG for these objectives.

The simulation results illustrate the output voltage, current, and power of the PV array, considering variations in solar radiation and temperature under standard operating conditions. Additionally, the simulation considers different load scenarios within the grid: full load, overload, and underload conditions. These varying load conditions introduce instability issues, such as voltage and frequency fluctuations by the intermitted nature of the renewable energy sources connected with the grid. However, the Virtual Synchronous Generator (VSG) control strategy effectively mitigates these instability problems. The results demonstrate that, under all load conditions, the VSG control successfully stabilizes the grid, verifying the effectiveness of the proposed control strategy.

B. Parameters of PV Based Micro Grid System

PV-based micro-grids often face instability challenges, including power fluctuations due to the variable nature of the PV modules and issues with frequency regulation and voltage stability, especially during sudden load changes. Since the PV source is expected to supply sufficient power to meet the load demands, accurately calculating the PV sizing is crucial. The desired power, voltage, and current levels are achieved by connecting individual PV modules in series and parallel configurations, similar to how batteries are arranged. The design equations for the PV modules are provided in Equations (1), (2), (3), and (4), and the corresponding parameters are outlined in Table 1. Additionally, the battery sizing calculations are presented in Table 2.

$$NM_P = \frac{I_{tot}}{I_M \times D_F} \quad (1)$$

$$I_{tot} = \frac{PV_{peakpower}}{SystemVoltage} \quad (2)$$

$$NM_S = \frac{V_S}{V_M} \quad (3)$$

$$NM_{tot} = NM_P \times NM_S \quad (4)$$

Where,

NM_P = Number of Parallel Module

NM_S = Number of Series Module

V_S = System Voltage

V_M = Module Rated Voltage

I_M = Module Rated Current

D_F = Module Derating Factor (0.98)

I_{tot} = Total PV Array Current

Table 1. PV Array Sizing for Case Study

Sr.No	**Parameter**	**Rating**	**Unit**	**Number**
1	Number of parallel modules	300	W	6
2	Number of series module	300	W	10
3	Total number of modules	300	W	60
4	Rated array current	75.123	A	-
5	Peak Power	36.296	kW	-

Table 2 . Battery Sizing for Case Study

Sr.No	Parameter	Rating	Unit	Number
1	System battery capacity	12,220	V, Ah	-
2	Number of parallel batteries	12,220	V, Ah	2
3	Number of series battery	12,220	V, Ah	20
4	Total number of batteries	12,220	V, Ah	40

5	Storage capacity	56,003	Ah	-

C. Regulation with Virtual Synchronous Generator Control Method

The Virtual Synchronous Generator (VSG) adjusts the output power of the PV panel and manages load consumption. A DC-DC Boost Converter regulates the unregulated DC voltage from the PV panel into a stable DC output. The bidirectional converter operates in buck mode when the PV output power exceeds the load demand, allowing the battery to charge with the excess energy. When the PV output is lower than the load demand, the converter switches to boost mode, and the battery discharges stored energy into the DC link. In the VSG system, an energy storage device is employed to absorb power fluctuations, ensuring system balance. A three-phase voltage source inverter serves as the interface between the DC link voltage and the load. During power imbalances, the VSG injects or absorbs power from the system as needed. The VSG control method also provides virtual inertia and damping properties, helping maintain the stability of the microgrid.

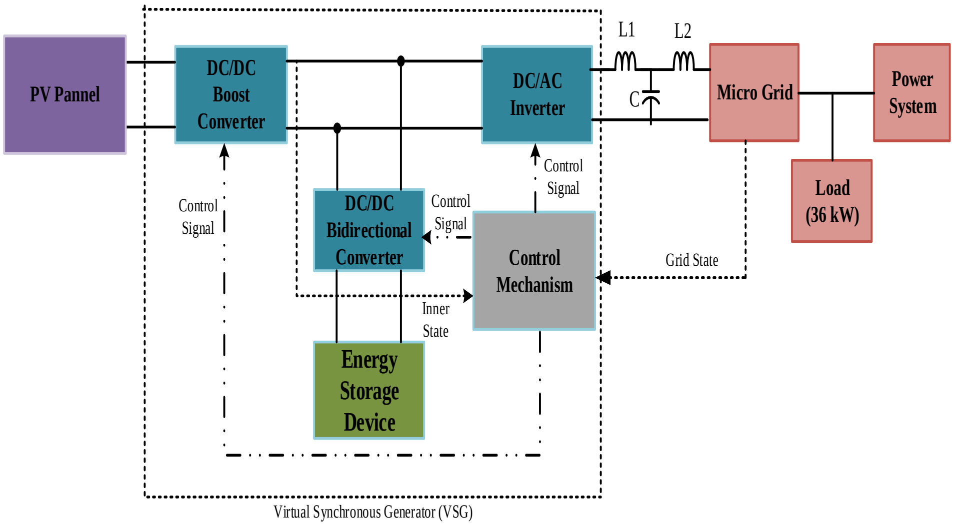

Figure 1. The Structure of VSG Control Method

D. Components of VSG

The VSG consists of power electronic converters, which include two power conversion stages: a DC-DC stage and a DC-AC stage, along with an energy storage device and a control scheme. The DC-DC stage includes both a DC-DC Boost Converter and a DC-DC Bidirectional Converter.

1. DC/DC Boost Converter

The voltage fluctuates due to the variable nature of the PV source. A DC-DC Boost Converter is used to regulate the unregulated DC voltage into a stable output. The output voltage of the DC-DC Boost Converter is higher than the input voltage. The design equations for the DC-DC Boost Converter are provided in Equations (5), (6), (7), and (8), and the corresponding parameters are listed in Table 3.

$$M_{V(max, min)} = \frac{V_0}{V_{S(min, max)}} \quad (5)$$

$$D_{(max, min)} = 1 - \frac{\eta_{con}}{M_{V(max, min)}} \quad (6)$$

$$\cdot L_{min} = \frac{R_{L(max)} \times D_{min}}{2 f_S} \left(1 - D_{min}\right)^2 \quad (7)$$

$$C_{min} = \frac{D_{max} V_0}{f_S R_{L(min)} V_{rccp}} \quad (8)$$

Where,

V_0= Output Voltage

V_S = Input Voltage

M_V = Transfer Function

D = Duty Cycle

f_s = Switching Frequency

R_L = Load Resistance

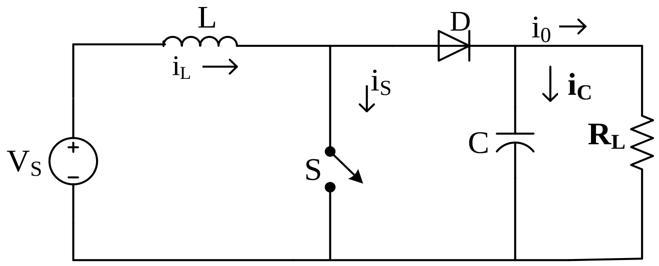

Figure 2. Circuit Diagram of Boost Converter [8]

Table 3. Parameters of Boost Converter

Sr. No	Parameter	Symbol	Rating	Unit
1	Mode	-	CCM	-
2	Minimum and maximum input voltage of converter	Vs	171~265	V
3	Output voltage of converter	V0	520	V
4	Switching frequency	fs	10k	Hz
5	Minimum inductance	L(min)	8.865m	H
6	Minimum capacitance	C(min)	72.405μ	F
7	Minimum and maximum duty Cycle	Dmin~Dmax	0.541346~0.704038	-

2. Bidirectional Converter

When the PV output power exceeds the load demand, the battery charges with the excess energy as the converter operates in buck mode. Conversely, when the PV output power is lower than the load demand, the battery discharges stored energy to the DC link while the converter operates in boost mode. The design equations for the DC Bidirectional Converter are provided in Equations (9), (10), (11), (12), and (13), and the corresponding parameters are listed in Table 4.

$$M_{V(buck,\ boost)} = \frac{V_{(L,H)}}{V_{(H,L)}} \tag{9}$$

$$D_{(2,1)} = 1 - \frac{\eta_{con}}{M_{V(buck,boost)}} \tag{10}$$

$$L = \frac{2}{27} \times \frac{R_L}{f_S} \tag{11}$$

$$C_1 = \frac{D_1}{2 f_S r_{C(max)}} \tag{12}$$

$$C_2 = \frac{D_2 V_L}{f_S R_L V_{rccp}} \tag{13}$$

Where,

V_H = High Voltage

V_L = low Voltage

D = Duty Cycle

f_s = Switching Frequency

η_{CON} = Converter Efficiency

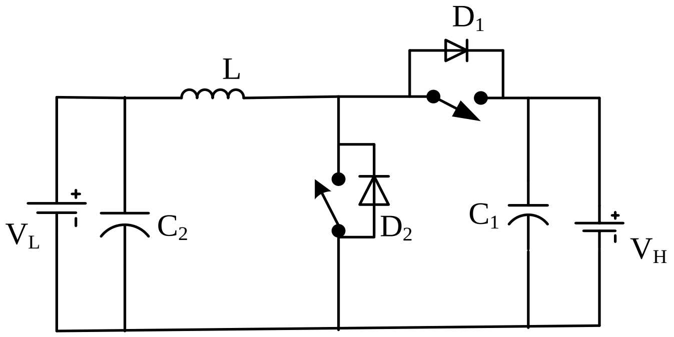

Figure 3. Circuit Diagram of Bidirectional Converter [9]

Table 4. Parameters of Bidirectional Converter

Sr. No	Parameter	Symbol	Rating	Unit
1	Low Voltage	VL	240	V
2	High Voltage	VH	520	V
3	Switching frequency	fs	10000	Hz
4	Inductor	L	4.7035m	H
5	Capacitor	C1	3597.6377µ	F

6	Capacitor	C2	58.89µ	F
7	Duty Cycle	D1 –D2	0.485-0.561	-

3. Inverter

When the generated power of the PV array exceeds 36 kW, a three-phase inverter is required. The inverter size should be 25-30% larger than the load consumption power. Hence, a 45 kW three-phase voltage source inverter is selected for the system. The PV array is connected to the AC grid, which is maintained at 400V, through a common DC/AC three-phase inverter. A Phase-Locked Loop (PLL) is used to track the phase angle and frequency of the grid voltage, which is needed for the dq-abc transformation block. The signal is then transformed back to the abc reference frame and sent to the PWM generator, which provides the pulses for the grid-connected inverter. Pulse Width Modulation (PWM) is used to control the switching of the inverter. The operational process of the inverter is illustrated in Figure 4.

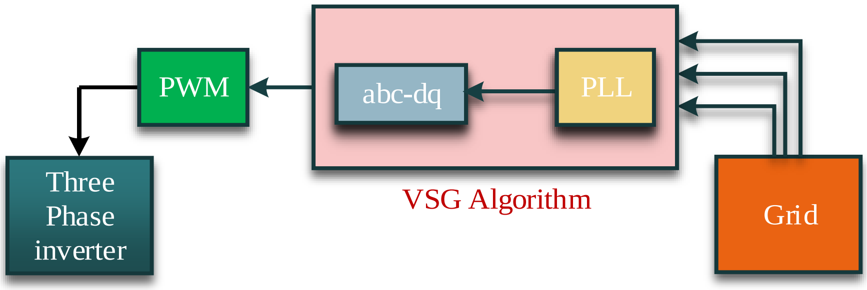

Figure 4. Schematic Diagram of Grid Connected Inverter

4. LCL Filter

Capacitors are used as filters to reduce the output voltage ripple of the converter, while inductors are employed to minimize harmonics in the inverter's output. Lower switching frequencies require larger capacitance and inductor sizes. However, higher switching frequencies result in increased switching losses, which reduces overall efficiency. The design equations for the LCL filter are provided in Equations (14), (15), and (16), with the corresponding parameters listed in Table 5.

$$L_1 = \frac{V_0}{8\Delta I_L f_S} \quad (14)$$

$$L_1 = 5L_2 \quad (15)$$

$$C = \frac{5\% P_{rated}}{3 \times 2\pi \times F \times (V_{rated})^2} \quad (16)$$

Where,

V_0 = Output Voltage

ΔI_L = Rated Current

F = System Frequency

f_s = Switching Frequency

P_{rated} = Rated Power

V_{rated} = Rated Voltage

Table 5. Parameters of LCL Filter

Sr. No	Parameter	Symbol	Rating	Unit
1	System frequency	F	50	Hz
2	switching frequency	fs	10K	Hz
3	Filter inductor size	L1	2.122m	H
4	Filter inductor size	L2	10.61m	H
5	Filter capacitor size	C	11.937µ	F

E. Modelling of System

For the modeling of the VSG-controlled microgrid connected to the PV system, MATLAB/SIMULINK software is used. The system's Simulink diagram represents the mathematical model of the VSG control strategy. Equations (17) to (32) describe the characteristics of the VSG model-based control. In this model, the characteristics of the Automatic Voltage Regulator (AVR) are also considered.

$$P^{\delta}VSG = \omega_{VSG} - \omega_{VSG0} \quad (17)$$

$$2H_{VSG}P\omega_{VSG} = (P_{PVin} - P_{PV}) - D_{VSG}(\omega_{VSG} - \omega_{VSG0}) \quad (18)$$

$$P_{PV} = V_{d,sys}\, i_{d,PV} + V_{q,sys}\, i_{q,PV} \quad (19)$$

$$P\,\Psi_{f,VSG} = v_{f,VSG} - r_{f,VSG}\, I_{f,VSG} \quad (20)$$

$$I_{f,VSG} = (\Psi_{f,VSG} + X_{md,VSG}\, i_{d,PV}) / X_{dA,VSG} \quad (21)$$

$$i_{d,PVref} = (e_{gq,VSG} - v_{q,PV}) / x'_{d,VSG} \quad (22)$$

$$i_{q,PVref} = v_{d,PV} / x_{q,VSG} \quad (23)$$

$$e_{gq,VSG} = K_{dA,VSG}\, \Psi_{f,VSG} \quad (24)$$

$$x_{d,VSG} = x_{a,VSG} + X_{md,VSG} \quad (25)$$

$$x'_{d,VSG} = x_{a,VSG} + X_{md,VSG} - X^2_{md,VSG} / X_{dA,VSG} \quad (26)$$

$$x_{q,VSG} = x_{a,VSG} + X_{mq,VSG} \quad (27)$$

$$K_{dA,VSG} = X_{md,VSG} / X_{dA,VSG} \quad (28)$$

$$X_{dA,VSG} = x_{f,VSG} / X_{md,VSG} \quad (29)$$

$$T_{A.VSG}\, P\, e_{f.VSG} = -\{(e_{f.VSG} - e_{f.VSG0}) + K_{A,VSG}(V_{sys} - V_{sys0})\} \quad (30)$$

$$e_{f,VSG} = (X_{md,VSG} / r_{f,VSG})\, v_{f,VSG} \quad (31)$$

$$V_{sys} = \sqrt{v_{d,sys}^2 + v_{q,sys}^2} \quad (32)$$

These equations are used the model of VSG control constructed as shown in figure 5.

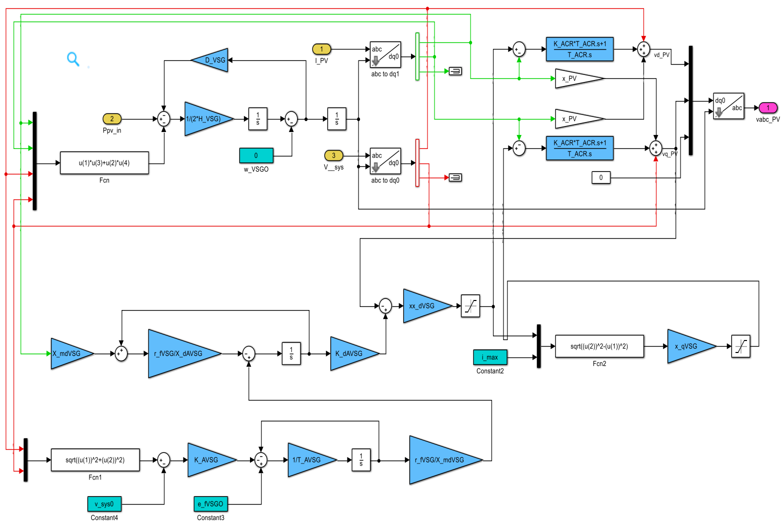

Figure 5. Simulink Model of Virtual Synchronous Generator (VSG)

The modeling of the VSG-controlled microgrid connected to the PV system is carried out using MATLAB/SIMULINK software. The model primarily consists of a PV array, DC-DC boost converter, DC-DC bidirectional converter, battery storage system, and the VSG control strategy. The Simulink model of the designed system, including the grid connection, is illustrated in Figure 6.

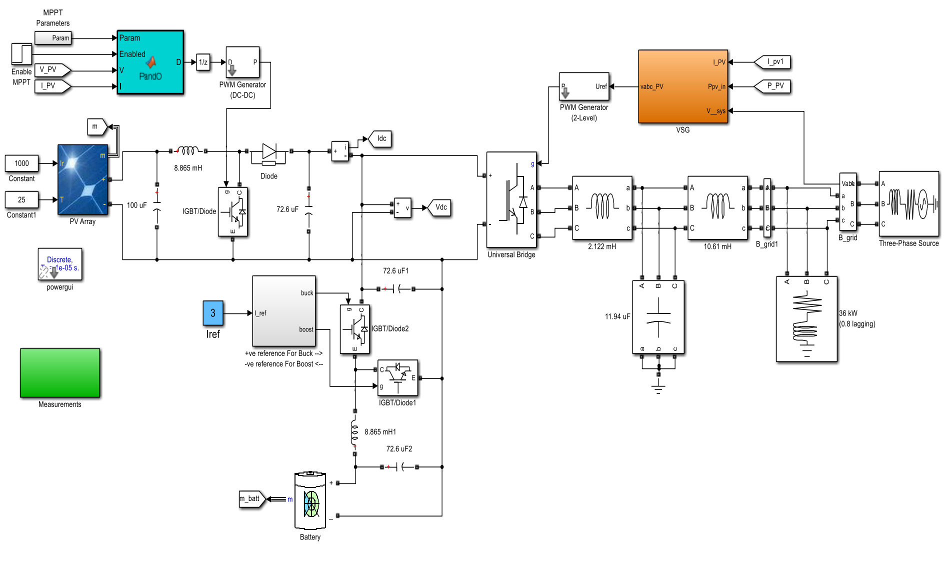

Figure 6. Simulink Model of VSG Controlled PV Based Micro-Grid System

F. Simulation Results and Analysis

This simulation considers variations in solar radiation while maintaining a constant temperature at standard operating conditions. The load varies between full load, overload, and underload conditions. The standard operating parameters for the PV array are an irradiance of 1000 W/m^2 and a temperature of 25°C. The simulation results, showing the output voltage, current, and power of the PV array, are presented in Figure 7.

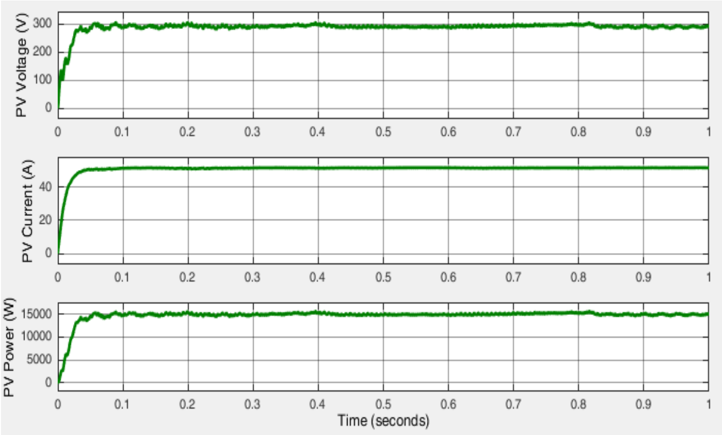

Figure 7. Simulation Results for PV Output Voltage, Current and Power

The DC-DC Boost Converter regulates the unregulated DC voltage into a stable DC output. The operation of the DC-DC Boost Converter is demonstrated in the simulation results. The output voltage, current, and power of the DC-DC Boost Converter are shown in Figure 8.

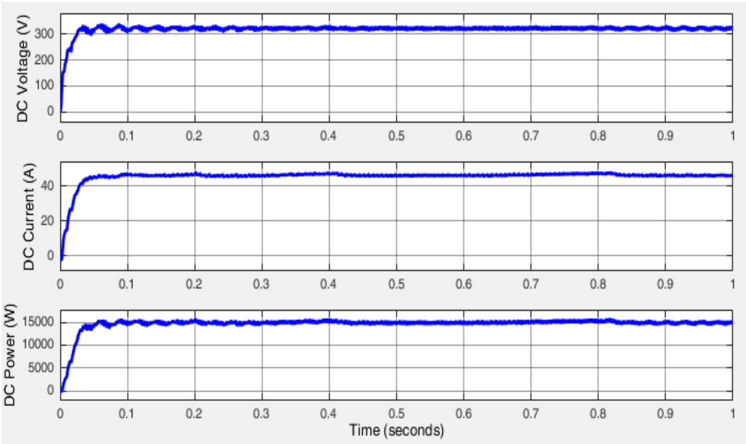

Figure 8. Simulation Results for DC Boost Converter Output Voltage, Current and Power

The three-phase voltage source inverter supplies AC voltage to the microgrid. The output voltage of the inverter remains stable under no-load conditions. The simulation results of the inverter's output voltage are shown in Figure 9.

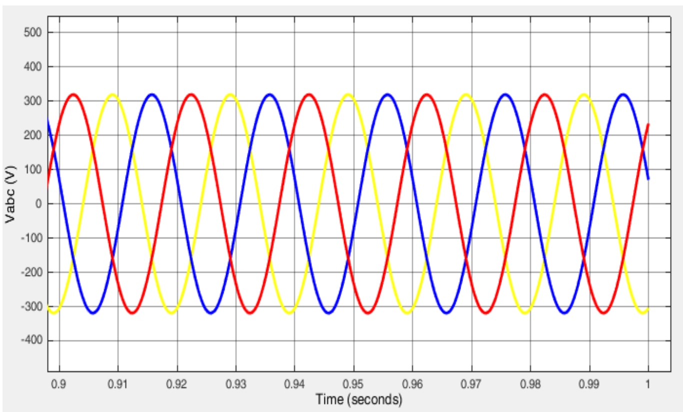

Figure 9. Simulation Results for Inverter Output Voltage

In the PV-based microgrid system operating at full load (36 kW), power fluctuations occur due to the variable nature of renewable energy sources (RESs), leading to degradation in frequency regulation. The simulation experiments demonstrate that the VSG control method effectively manages voltage and frequency, showcasing strong self-adjusting capabilities. The simulation results are presented in Figures 10 and 11.

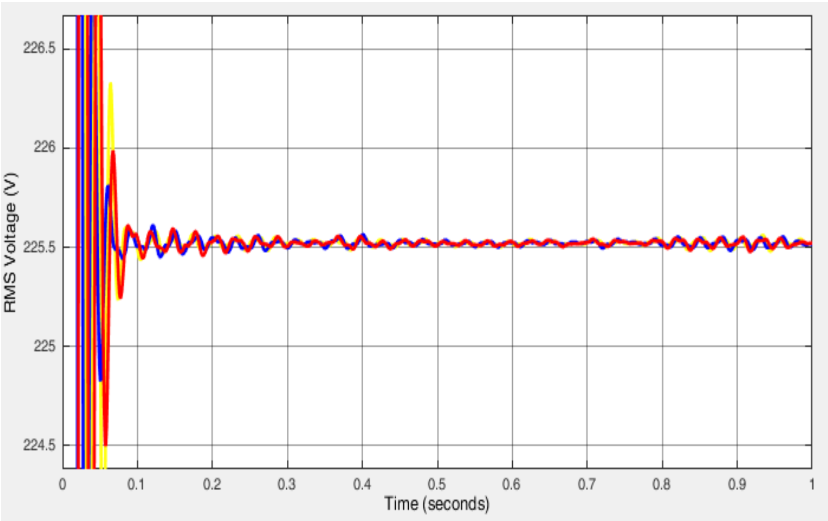

Figure 10. Simulation Results for System RMS Voltage of Inverter

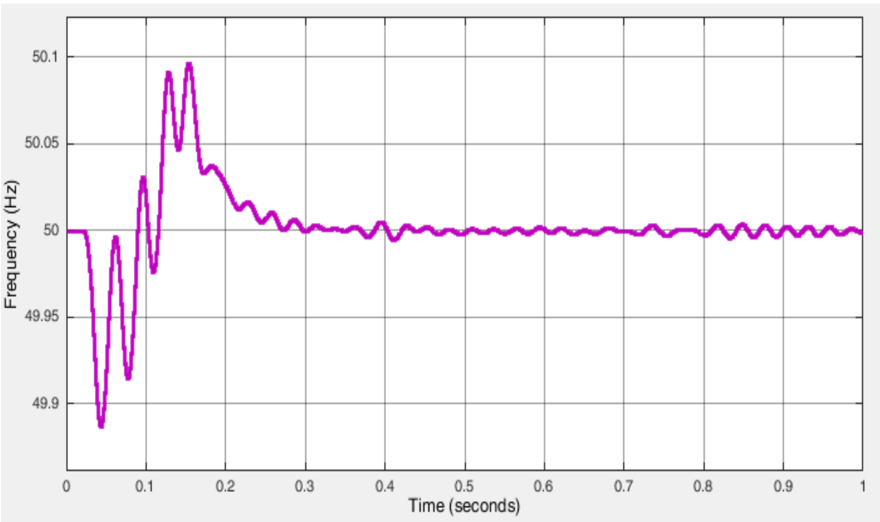

Figure 11. Simulation Results for System Frequency

When a 10-kW load is added to the full load (36 kW) in the PV-based microgrid system, the total load consumption rises to 46 kW, resulting in an insufficient supply from the PV source. This scenario represents an overload condition. During power imbalances in the microgrid, the actual simulation experiments indicate that the voltage remains stable across different load configurations, typically achieving stability within a few seconds. The time required to reach a stable voltage state varies with changes in load, but it generally stabilizes within approximately 0.2 seconds. The simulation results are shown in Figures 12 and 13.

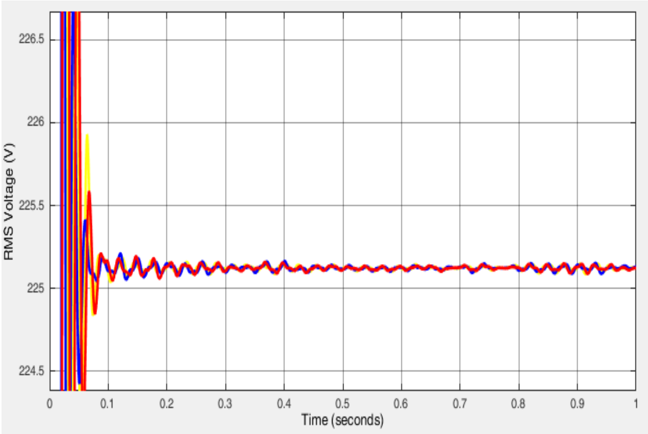

Figure 12. Simulation Results for System RMS Voltage of Overload Condition

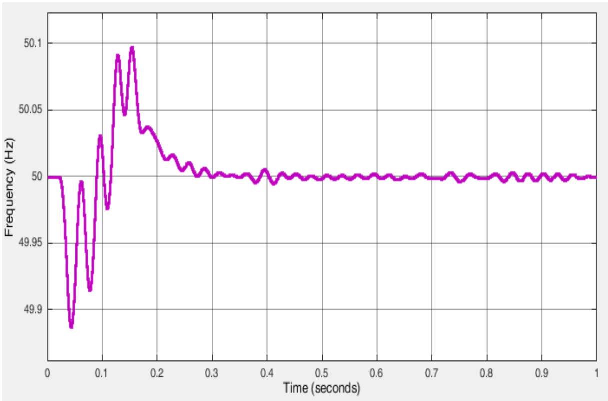

Figure 13. Simulation Results for System Frequency of Overload Condition

Under load conditions, the voltage rises due to reverse power from PV generation, accompanied by voltage fluctuations and system frequency deviations caused by the variable nature of PV energy. The actual experimental simulation results demonstrate that the VSG control strategy effectively addresses these instability issues, achieving stabilization within 0.2 seconds. Additionally, the frequency of the entire system remains stable at 50 Hz. The simulation results are presented in Figures 14 and 15.

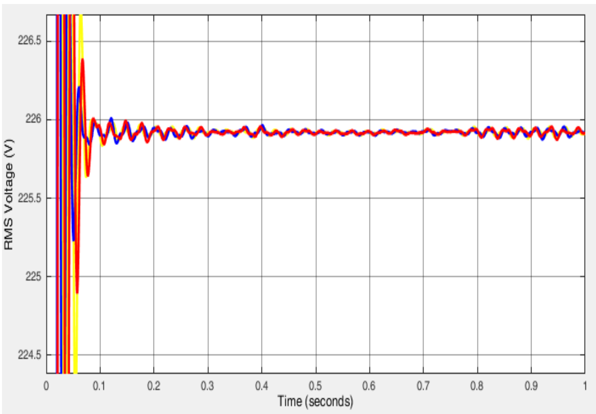

Figure 14. Simulation Results for System RMS Voltage of under load Condition

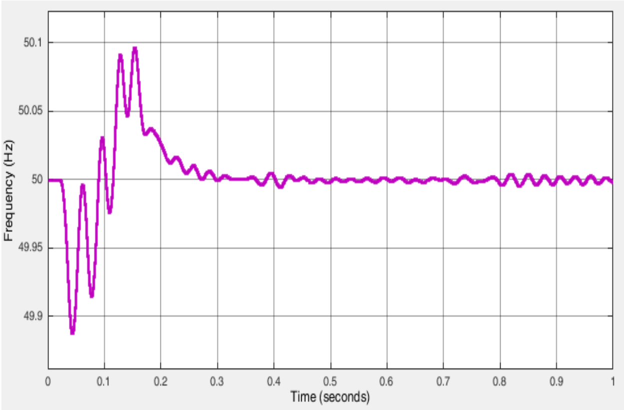

Figure 15. Simulation Results for System Frequency of Under load Condition

G. Conclusion

This paper presents the proposed VSG control method, highlighting its critical characteristic of quickly counteracting power system deviations to support frequency stability. In the event of a power imbalance, the VSG can inject or absorb power from the system, effectively mitigating fluctuations within a matter of seconds.

The simulation demonstrates the effectiveness of the system stabilization under various load conditions, including under-load (26 kW), full-load (36 kW), and over-load (46 kW) scenarios. The phase voltage and frequency remain stable at the designed values of 230 V and 50 Hz, respectively. Thus, the VSG model is suitable for maintaining voltage and frequency stability in the integration of large PV systems into the power grid. However, a notable disadvantage is the requirement for additional electronic devices and control systems to regulate this setup.

H. References

[1] Virtual Synchronous Generator , J Driesen , K. Vesscher, Member IEEE 2015.
[2] Virtual Synchronous Generator Based Inverter Control Method for Distributed Generation Systems , IEEE 2015.
[3] An improved Virtual Synchronous Generator Algorithm for system stability enhancement . IEEE 2015.
[4] Application of VSG Technology in Microgrid , IEEE 2016.
[5] Integration of Distributed Energy Resources in Power System Handbook , Toshifumi Ise , Hassan Bevrani , University of Kurdistan, Sanandaj, Iran 2016.
[6] Microgrid Dynamic and Control, First Edition , Hassan Bevrani , Bruno Francois and Toshefumi Ise , 2017.
[7] Virtual Synchronous Generator : AN OVERVIEW, NIJOTECH, 2019
[8] Power Electronic Handbook, third Edition , Muhammad H.Rashid.